

Full Length Research Paper

Peristaltic flow of a Prandtl fluid model in an asymmetric channel

Noreen Sher Akbar^{1*}, S. Nadeem¹ and Changhoon Lee²

¹Department of Mathematics, Quaid-i-Azam University 45320, Islamabad 44000, Pakistan.

²Department of Computational Sciences and Engineering, Yonsei University Seoul, Korea.

Accepted 14 December, 2011

The peristaltic flow of a Prandtl fluid in an asymmetric channel has been investigated both analytically and numerically. This is the first article describing feature of Prandtl fluid model in peristaltic literature. The governing equations for the proposed Prandtl fluid model are derived in Cartesian coordinates system. Asymmetric channel have been taken into account for the present analysis. Longwave length and low Reynolds number assumptions have been utilized to simplify the problem. Regular perturbation method and shooting method were used to get the analytical and numerical solutions for velocity, stream function and pressure gradient. Some special cases of this problem are compared with the existing literature. The effects of physical parameters on the velocity, pressure rise and streamlines are examined by plotting graphs.

Key words: Peristaltic flow, Prandtl fluid model, asymmetric channel, perturbation solution, numerical solution.

INTRODUCTION

Peristalsis is a radially symmetrical contraction of muscles which propagates in a way down a muscular tube. This process is quite important for fluid transport in living organisms and industry. Blood pumps in dialysis and heart lung machine works because of the peristaltic phenomena. Further, peristalsis occurs in swallowing food through the esophagus, chyme motion in the gastrointestinal tract, in the vasomotion of small blood vessels such as venules, capillaries and arterioles, urine transport from kidney to bladder, in sanitary fluid transport, transport of corrosive fluids, a toxic liquid transport in the nuclear industry etc. Latham (1996) and Jaffrin and Shapiro (1971) presented the initial research work on the peristalsis. They discussed the fluid motion in a peristaltic pump. Non-linear peristaltic flow of a fourth grade fluid in an inclined asymmetric channel was discussed by Haroun (2007). Mekheimer (2008) analyzed the effects of the induced magnetic field on peristaltic flow of a couple stress fluids. Influence of heat transfer on peristaltic transport of a Johnson-Segalman fluid in an

inclined asymmetric channel was observed by Nadeem and Akbar (2008). Yildirim and Sezer (2010) discussed the effects of partial slip on the peristaltic flow of a magnetohydrodynamic (MHD) Newtonian fluid in an asymmetric channel. During the past few years, many authors have discussed the study of peristaltic flow of different non-Newtonian fluid models. Mention may be made to the works of Mekheimer and Elmaboud (2008), Nadeem and Akbar (2010), Srinivas et al. (2009), Akbar et al. (2011) and Hayat et al. (2008).

Most of the fluids in nature possess non-Newtonian characteristics. Non-Newtonian fluids change their viscosity or flow behaviour under stress. Not all non-Newtonian fluids behave in the same way when stress is applied; some become more solid while others more fluid. Some non-Newtonian fluids react as a result of the amount of stress applied, while others react as a result of the length of time that stress is applied. Recently, a most important article of stress strain relationship for viscous-inelastic non-Newtonian fluids has been discussed by Patel and Timol (2010). They have made a detail analysis for some important non-Newtonian fluids. According to them, academic curiosity and practical applications have generated considerable interest in finding the solutions of

*Corresponding author. E-mail: noreensher@yahoo.com.

differential equations governing the motion of non-Newtonian fluids. Prandtl fluid model is also a non-Newtonian fluid model, which is given in the study of Patel and Timol (2010). Prandtl fluid model has all the characteristics of non-Newtonian fluid. Some other important articles related to the topic are cited in the reference (Rico Garcia, 2011; Ellahi, 2009; Okosun and Makinde, 2011).

Thus, the purpose of the current study is to examine the peristaltic flow of a Prandtl fluid in an asymmetric channel. The study of Prandtl model for peristaltic flow problems are not explored so far. Therefore, to fill this gap in the present analysis, we have discussed the peristaltic flow of Prandtl fluid model in an asymmetric channel. The governing equations of Prandtl fluid model have been developed and then simplified under the assumptions of longwave length and low Reynolds number approximation. Expressions of stream function, longitudinal pressure gradient and pressure rise have been computed using perturbation technique. To validate the perturbation results, numerical solutions have been calculated using shooting method. Comparisons have been made through tables and figures. Graphical results have been presented and analyzed for various parameters entering into the present analysis.

MATHEMATICAL DEVELOPMENT

Consider an incompressible Prandtl fluid in an asymmetric channel of width $d_1 + d_2$. The channel has a sinusoidal wave propagating with constant speed c on the channel walls induces the flow. The asymmetric of the channel is due to different amplitudes. The wall surfaces are selected to satisfy the following expressions:

$$Y = H_1 = d_1 + a_1 \cos \left[\frac{2\pi}{\lambda} (X - ct) \right], \tag{1}$$

$$Y = H_2 = -d_2 - b_1 \cos \left[\frac{2\pi}{\lambda} (X - ct) + \phi \right].$$

In Equations 1, a_1 and b_1 are the waves amplitudes, λ is the wave length, $d_1 + d_2$ is the channel width, c is the wave speed, t is the time, X is the direction of wave propagation and Y is perpendicular to X . The phase difference ϕ varies in the range $0 \leq \phi \leq \pi$. When $\phi = 0$, then symmetric channel with waves out of phase can be described and for $\phi = \pi$, the waves are in phase. Moreover, a_1, b_1, d_1, d_2 and ϕ satisfies the following relation:

$$a_1^2 + b_1^2 + 2a_1b_1 \cos \phi \leq (d_1 + d_2)^2.$$

in the laboratory frame, the following equations can govern the flow:

$$\frac{\partial \bar{U}}{\partial \bar{X}} + \frac{\partial \bar{V}}{\partial \bar{Y}} = 0, \tag{2}$$

$$\rho \left(\frac{\partial \bar{U}}{\partial t} + \bar{U} \frac{\partial \bar{U}}{\partial \bar{X}} + \bar{V} \frac{\partial \bar{U}}{\partial \bar{Y}} \right) = -\frac{\partial P}{\partial \bar{X}} + \frac{\partial}{\partial \bar{X}} (\bar{S}_{\bar{X}\bar{X}}) + \frac{\partial}{\partial \bar{Y}} (\bar{S}_{\bar{X}\bar{Y}}), \tag{3}$$

$$\rho \left(\frac{\partial \bar{V}}{\partial t} + \bar{U} \frac{\partial \bar{V}}{\partial \bar{X}} + \bar{V} \frac{\partial \bar{V}}{\partial \bar{Y}} \right) = -\frac{\partial P}{\partial \bar{Y}} + \frac{\partial}{\partial \bar{X}} (\bar{S}_{\bar{X}\bar{Y}}) + \frac{\partial}{\partial \bar{Y}} (\bar{S}_{\bar{Y}\bar{Y}}), \tag{4}$$

where \bar{U} and \bar{V} are the velocities in the \bar{X} and \bar{Y} directions in fixed frame, ρ is the density and \bar{P} is the pressure.

The coordinates, velocity components and pressure between fixed and wave frames are related by the following transformations:

$$\bar{x} = \bar{X} - ct, \bar{y} = \bar{Y}, \bar{u} = \bar{U} - c, \bar{v} = \bar{V}, p(\bar{x}) = P(\bar{X}, t), \tag{5}$$

in which $(\bar{x}, \bar{y}), (\bar{u}, \bar{v})$ and \bar{p} are the coordinates, velocity components and pressure in the wave frame, respectively.

Expression of an extra stress tensor for Prandtl fluid is given by Patel and Timol. (2010)

$$\bar{S} = \frac{A \sin^{-1} \left\{ \frac{1}{C} \left[\left(\frac{\partial \bar{u}}{\partial \bar{y}} \right)^2 + \left(\frac{\partial \bar{v}}{\partial \bar{x}} \right)^2 \right]^{\frac{1}{2}} \right\}}{\left[\left(\frac{\partial \bar{u}}{\partial \bar{y}} \right)^2 + \left(\frac{\partial \bar{v}}{\partial \bar{x}} \right)^2 \right]^{\frac{1}{2}}} \frac{\partial \bar{u}}{\partial \bar{y}}, \tag{6}$$

in which \bar{S} is the extra stress tensor, A and C are material constant of Prandtl fluid model.

Making use of velocity stream function relation and non-dimensional quantities, we have:

$$u = \frac{\partial \Psi}{\partial y}, v = -\delta \frac{\partial \Psi}{\partial x}, \tag{7}$$

$$x = \frac{2\pi \bar{x}}{\lambda}, y = \frac{\bar{y}}{d_1}, u = \frac{\bar{u}}{c}, v = \frac{\bar{v}}{c}, t = \frac{2\pi \bar{t}}{\lambda}, \delta = \frac{2\pi d_1}{\lambda}, d = \frac{d_2}{d_1}, P = \frac{2\pi d_1^2 P}{\mu c \lambda}, \tag{8}$$

$$h_1 = \frac{\bar{h}_1}{d_1}, h_2 = \frac{\bar{h}_2}{d_2}, Re = \frac{\rho c d_1}{\mu}, a = \frac{a_1}{d_1}, b = \frac{a_2}{d_1}, d = \frac{d_2}{d_1}, S = \frac{\bar{S} d_1}{\mu c}.$$

Equations 2 to 6 after using the long wavelength and low Reynolds number approximation take the following form. We finally obtain the following system of equations:

$$\frac{\partial^2}{\partial y^2} \left[\alpha \frac{\partial^2 \Psi}{\partial y^2} + \beta \left(\frac{\partial^2 \Psi}{\partial y^2} \right)^3 \right] = 0, \tag{9}$$

$$\frac{dP}{dx} = \frac{\partial}{\partial y} \left[\alpha \frac{\partial^2 \Psi}{\partial y^2} + \beta \left(\frac{\partial^2 \Psi}{\partial y^2} \right)^3 \right], \quad (10)$$

where

$$\alpha = \frac{A}{\mu C}, \quad \beta = \frac{\alpha c^2}{C^2 d_1}.$$

Corresponding boundary conditions for asymmetric channel in non-dimensional form take the following form:

$$\Psi = \frac{F}{2}, \quad \frac{\partial \Psi}{\partial y} = -1, \quad \text{at } y = h_1 = 1 + a \cos x, \quad (11)$$

$$\Psi = -\frac{F}{2}, \quad \frac{\partial \Psi}{\partial y} = -1, \quad \text{at } y = h_2 = -d - b \cos(x + \phi). \quad (12)$$

The time mean Q in the wave frame are defined as:

$$Q = F + 1 + d. \quad (13)$$

SOLUTION OF THE PROBLEM

Series expressions

We note that the resulting Equation 9 is highly nonlinear. Hence, the solutions for small Prandtl parameter β can be expressed as:

$$\Psi = \Psi_0 + \beta \Psi_1 + O(\beta^2), \quad (14)$$

$$\frac{dP}{dx} = \frac{dP_0}{dx} + \beta \frac{dP_1}{dx} + O(\beta^2), \quad (15)$$

$$F = F_0 + \beta F_1 + O(\beta^2), \quad (16)$$

Substituting Equations 14, 15 and 16 into Equations 9 to 12 and then solving the resulting systems, we finally obtain:

$$\Psi(x, y) = A_1 + A_2 y + A_3 y^2 + A_4 y^3 + \beta \left((-18A_3 A_4^2 y^4 / \alpha) - (54A_4^3 y^5 / 5\alpha) + A_5 + A_6 y + A_7 y^2 + A_8 y^3 \right), \quad (17)$$

$$\frac{dP}{dx} = -\frac{2(F + h_1 - h_2)}{(h_1 - h_2)^3} + \beta \left(\frac{18(10A_3 A_4^2 (h_1 + h_2) + 9A_4^3 (h_1^2 + h_2^2) + 12A_4^3 h_1 h_2)}{5\alpha} \right), \quad (18)$$

where

$$\begin{aligned} A_1 &= -\frac{Fh_1^3 - 3Fh_1^2 h_2 - 2h_1^3 h_2 - 3Fh_1 h_2^3 + Fh_2^3 + 2h_1 h_2^3}{2(h_1 - h_2)^3}, \\ A_2 &= -\frac{h_1^3 + 6Fh_1 h_2 + 3h_1^2 h_2 - 3h_1 h_2^2 - h_2^3}{(h_1 - h_2)^3}, \\ A_3 &= \frac{3(F + h_1 - h_2)(h_1 + h_2)}{(h_1 - h_2)^3}, \quad A_4 = -\frac{2(F + h_1 - h_2)}{(h_1 - h_2)^3}, \\ A_5 &= \frac{18(5A_3 A_4^2 h_1^2 h_2^2 + 6A_4^3 h_1^3 h_2^3 + 6A_4^3 h_1^2 h_2^3)}{5\alpha}, \\ A_6 &= \frac{18(10A_3 A_4^2 h_1 h_2 (h_1 + h_2) + 12A_4^3 h_1 h_2 (h_1^2 + h_2^2) + 21A_4^3 h_1^2 h_2^2)}{5\alpha}, \\ A_7 &= -\frac{18(5A_3 A_4^2 (h_1^2 + h_2^2) + 6A_4^3 (h_1^3 + h_2^3) + 20A_3 A_4^2 h_1 h_2 + 24A_4^3 h_1 h_2 (h_1 + h_2))}{5\alpha}, \\ A_8 &= \frac{18(10A_3 A_4^2 (h_1 + h_2) + 9A_4^3 (h_1^2 + h_2^2) + 12A_4^3 h_1 h_2)}{5\alpha}. \end{aligned}$$

and the dimensionless pressure rise ΔP is defined as:

$$\Delta P = \int_0^1 \left(\frac{dP}{dx} \right) dx. \quad (19)$$

Numerical solutions

Here, the problem consisting of Equations 9, 11 and 12 are also solved numerically by employing shooting method. The numerical solutions are also compared with the perturbation solution. The

difference between the values of two solutions is shown in Tables 1 and 2.

RESULTS AND DISCUSSION

In this section, we have examined the pressure rise, pressure gradient, velocity and streamlines for Prandtl fluid model through graphs. In order to analyze the pressure rise per wavelength, numerical integration has been carried out. The pressure rise against volume flow

Table 1. Comparison of velocity profile for fixed $a=0.1$, $b=0.5$, $d=1$, $\phi=0.2$, $Q=2$, $x=1$, $\alpha=1.5$, $\beta=0.2$.

y	$u(x,y)$ Perturbation solution	$u(x,y)$ Numerical solution
-1.5	-1.0000	-1.0000
-1.2	-0.5235	-0.5236
-0.9	0.0045	0.0045
-0.6	0.4225	0.4226
-0.3	0.6345	0.6345
0.0	0.5961	0.5962
0.3	0.3154	0.3154
0.6	-0.1481	-0.1481
0.9	-0.6827	-0.6827
1.2	-1.0000	-1.0000

Table 2. Comparison of velocity profile for fixed $a=0.1$, $b=0.5$, $d=1$, $\phi=0.2$, $Q=2$, $x=1$, $\alpha=1.5$, $\beta=0.2$.

y	$u(x,y)$ for present work when $\alpha=1$, $\beta=0$	$u(x,y)$ (Yildirim and Sezer, 2010) when $M=0$, $\beta=0$
-1.5	-1.0000	-1.0000
-1.2	-0.4034	-0.4034
-0.9	0.0555	0.0555
-0.6	0.3533	0.3533
-0.3	0.4902	0.4902
0.0	0.4659	0.4659
0.3	0.2808	0.2808
0.6	-0.0653	-0.0653
0.9	-0.5725	-0.5725
1.2	-1.0000	-1.0000

rate is shown in Figures 1a to d. It is observed that the pressure rise and volume flow rate are giving opposite behaviour. From Figures 1a to 1d, it is also noticed that in pumping region ($\Delta P > 0$), the pressure rise increases with the increase of Prandtl fluid parameter β and amplitude b . The pressure rise decreases when Prandtl fluid parameter α and phase difference ϕ are increased. Figures 1a to d also show that in the augmented pumping region for ($\Delta P < 0$), the pressure rise decreases when we increase Prandtl fluid parameter β and amplitude b . However, the pressure rise increases when Prandtl fluid parameter α and phase difference ϕ are increased. Free pumping region holds when ($\Delta P = 0$). Variations of Prandtl fluid parameter β , Prandtl fluid parameter α and flow Q on the velocity profile are shown in the Figures 2a to c. Figures 2a and c depicts that the behavior of velocity

near the channel walls and at center are not similar in view of the Prandtl fluid parameters α and β . The velocity field increases with the increase of β in the region $y \in [0.4, -0.6]$ while velocity field decreases in the other region; by increasing α , velocity field decreases in the region $y \in [0.4, -0.6]$ and increases in rest of the region. The velocity for the flow rate Q is plotted in Figure 2c. It is found that the velocity field increases with an increase in the flow rate.

Figures 3a to d show the pressure gradient for different values of α , β , a and b . The magnitude of pressure gradient increases with increase in β , a and b . Note that the pressure gradient decreases by increasing α . It is also observed that the maximum pressure gradient occurs when $x=0.48$ and near the channel walls pressure gradient is small. It means flow can easily pass in the middle of the channel.

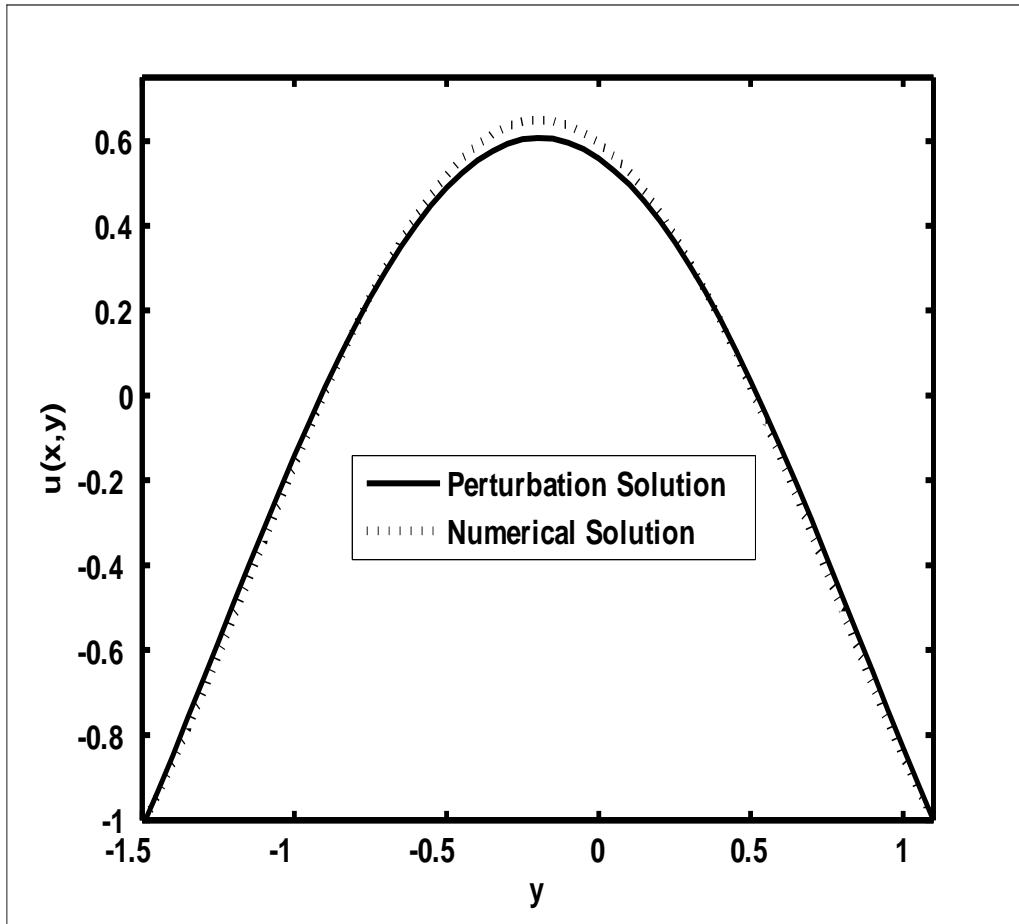


Figure 1. Comparison of velocity profile for fixed $a = 0.1$, $b = 0.5$, $d = 1$, $\phi = 0.2$, $Q = 2$, $x = 1$, $\alpha = 1.5$, $\beta = 0.2$.

The trapping for different values of α and β are shown in the Figures 4a to d and 5a to d. As shown in Figure 4a and b, the size of the trapping bolus decreases with an increase in α (in the upper part of the channel) and size of trapping bolus increases in the lower parts of the channel when we increased α . Figure 4a and d show that the size of trapping bolus decreases with an increase in β in the upper and lower parts of the channel, while the number of the trapping bolus increases in the upper half of the channel.

In order to make the comparison of the present and previous results, we prepared Tables 1 and 2.

Conclusion

The present study looks at the peristaltic flow of a Prandtl fluid in an asymmetric channel. The main points of the performed analysis are as follows:

1. The qualitative behaviors of Prandtl fluid parameter β

and amplitude b on the pressure rise are similar.

2. The pressure rise increases when we increase Prandtl fluid parameter β and amplitude b .

3. Pressure rise decreases with an increase in Prandtl fluid parameter α and phase difference ϕ

4. The effects of β and Q on the velocity profile are similar in qualitative sense.

5. Velocity profile decreases in view of increase in α .

6. The magnitude of pressure gradient increases with the increase in β , a and b .

7. The qualitative behaviour of α on magnitude of pressure gradient is not similar as compared to the β , a and b .

8. The size of the trapping bolus decreases with an increase in α (in the upper part of the channel) and size of trapping bolus increases in the lower parts of the channel when we increased α .

9. The size of trapping bolus decreases with an increase

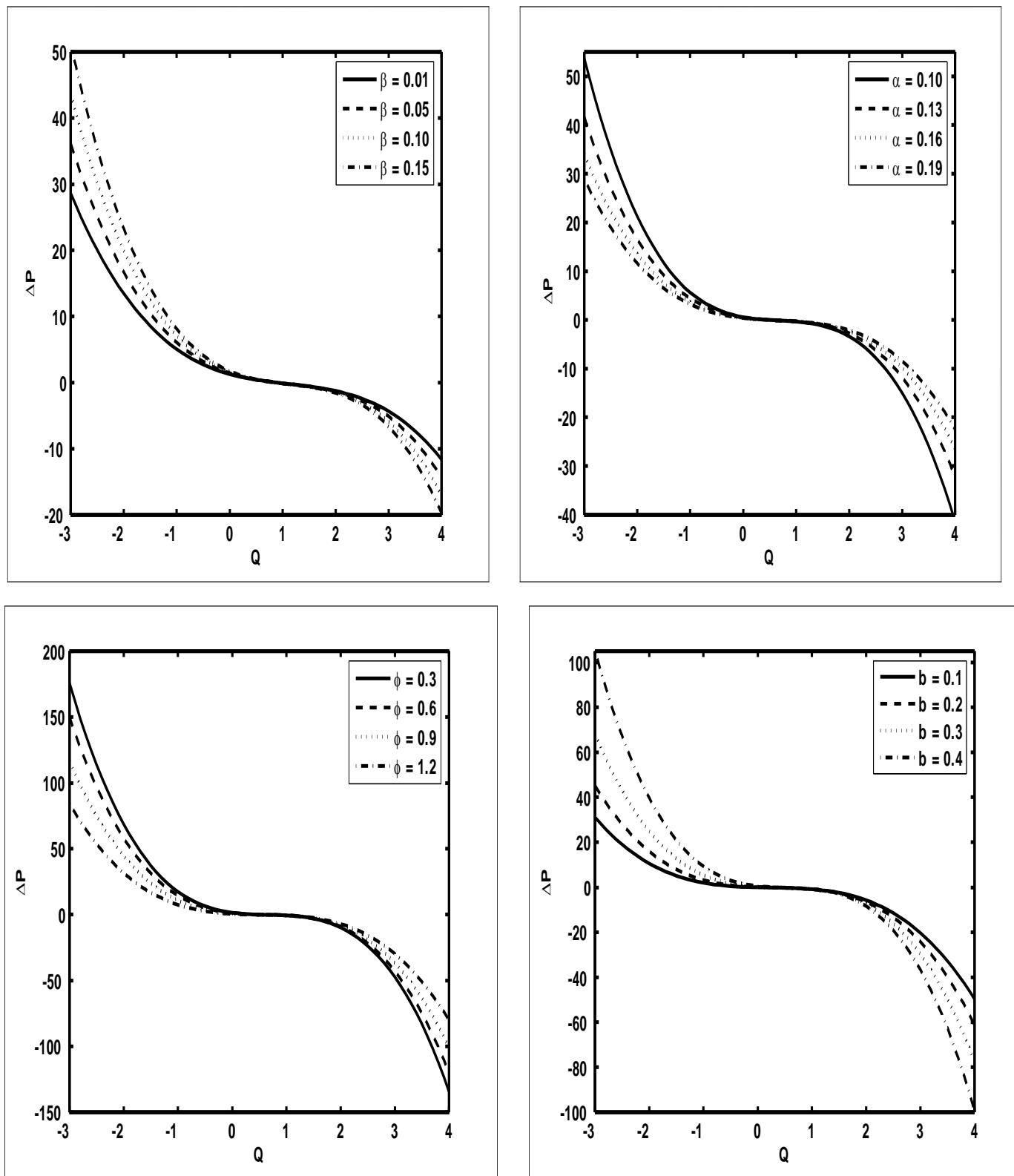


Figure 2. Variation of pressure rise versus flow rate for (a) $\alpha = 0.4$, $a = 0.7$, $b = 0.5$, $d = 1$, $\phi = 0.1$. (b) $\beta = 0.05$, $a = 0.3$, $b = 0.5$, $\phi = 0.3$, $d = 1$. (c) $\beta = 0.05$, $a = 0.3$, $b = 0.5$, $\alpha = 0.03$, $d = 1$. (d) $\beta = 0.05$, $a = 0.3$, $d = 1$, $\phi = 0.5$, $\alpha = 0.03$.

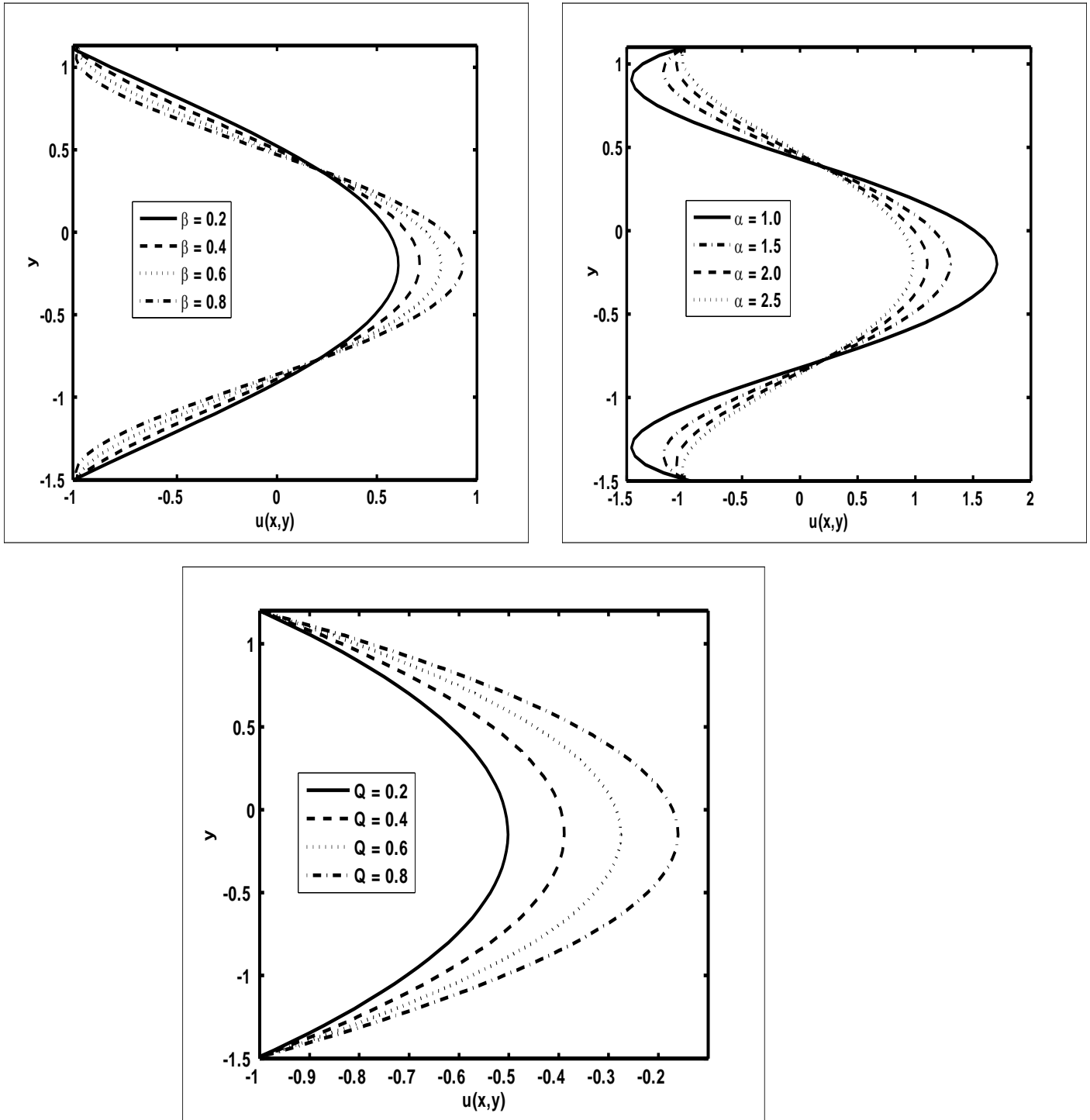


Figure 3. Variation of velocity profile for (a) $a=0.1, d=1, b=0.5, \phi=0.2, Q=2, \alpha=1.5, x=1$. (b) $a=0.1, d=1, b=0.5, \phi=0.2, Q=2, \beta=1.5, x=1$. (c) $\beta=0.1, d=1, b=0.5, \phi=0.2, a=0.2, \alpha=1.5, x=1$.

in β in the upper and lower parts of the channel, while the number of the trapping bolus increases in the upper half of the channel.

ACKNOWLEDGEMENT

The author Changhoon Lee is thankful to Younsei University South Korea for providing grant under WCU

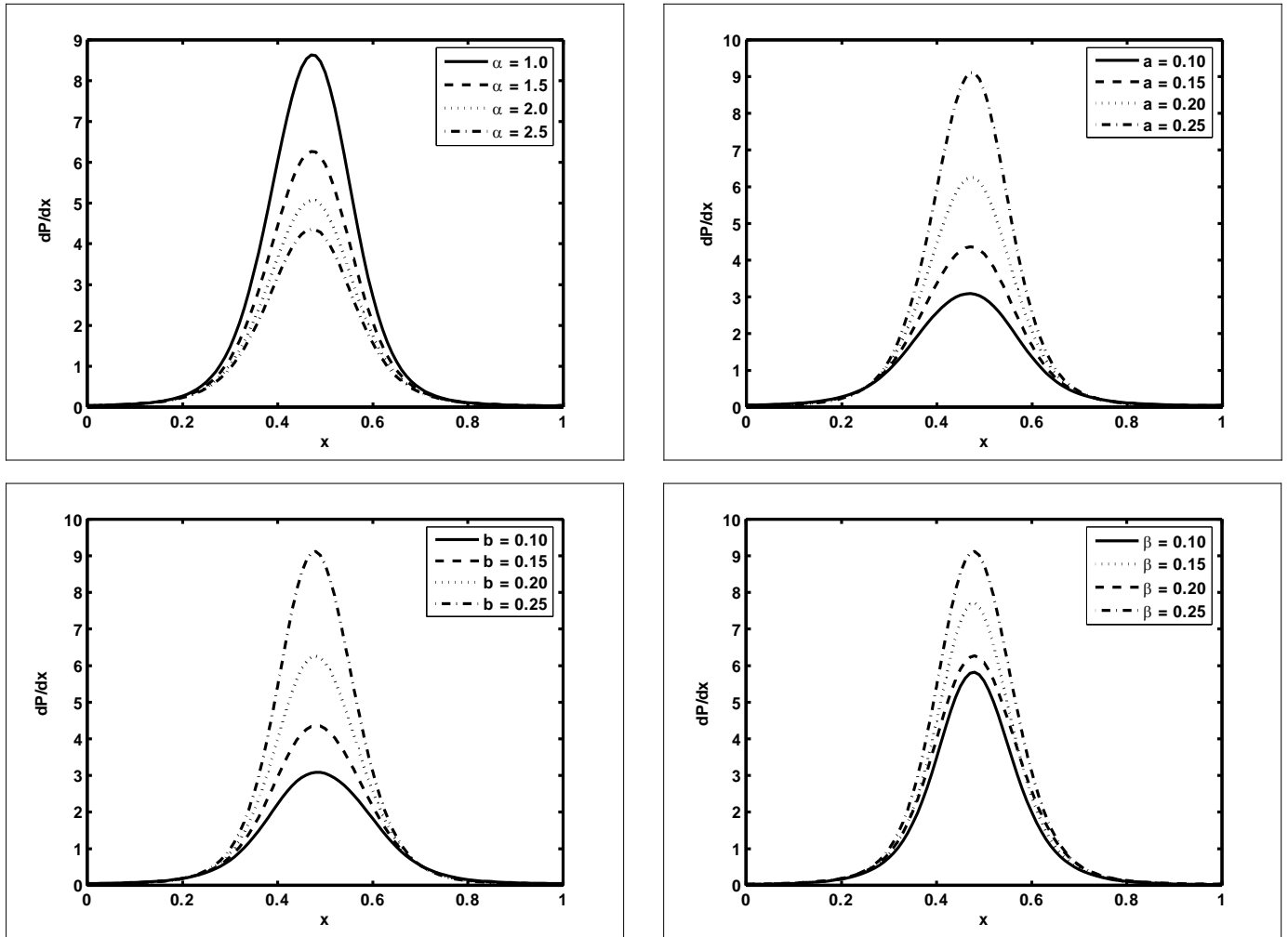
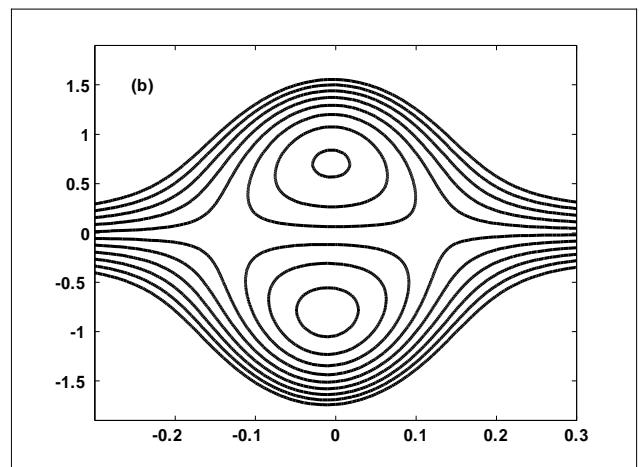
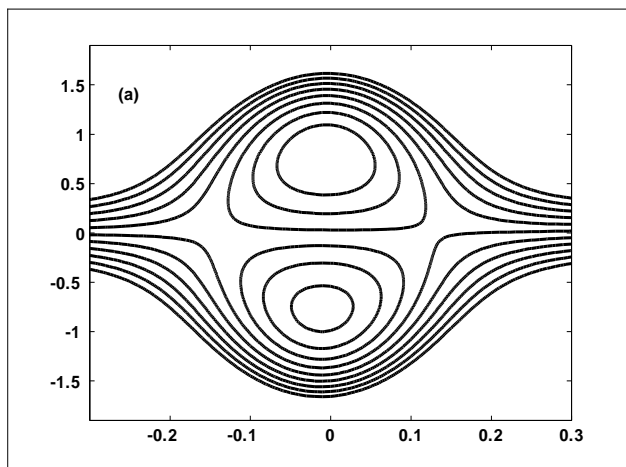


Figure 4. Variation of pressure gradient for (a) $\beta = 0.03$, $a = 0.2$, $d = 1$, $b = 0.5$, $Q = -1$. (b) $\beta = 0.3$, $\alpha = 1.5$, $d = 1$, $b = 0.5$, $Q = -1$, $\phi = 0.3$. (c) $\beta = 0.3$, $\alpha = 1.5$, $d = 1$, $a = 0.5$, $Q = -1$, $\phi = 0.3$. (d) $b = 0.3$, $\alpha = 1.5$, $d = 1$, $a = 0.5$, $Q = -1$, $\phi = 0.3$.



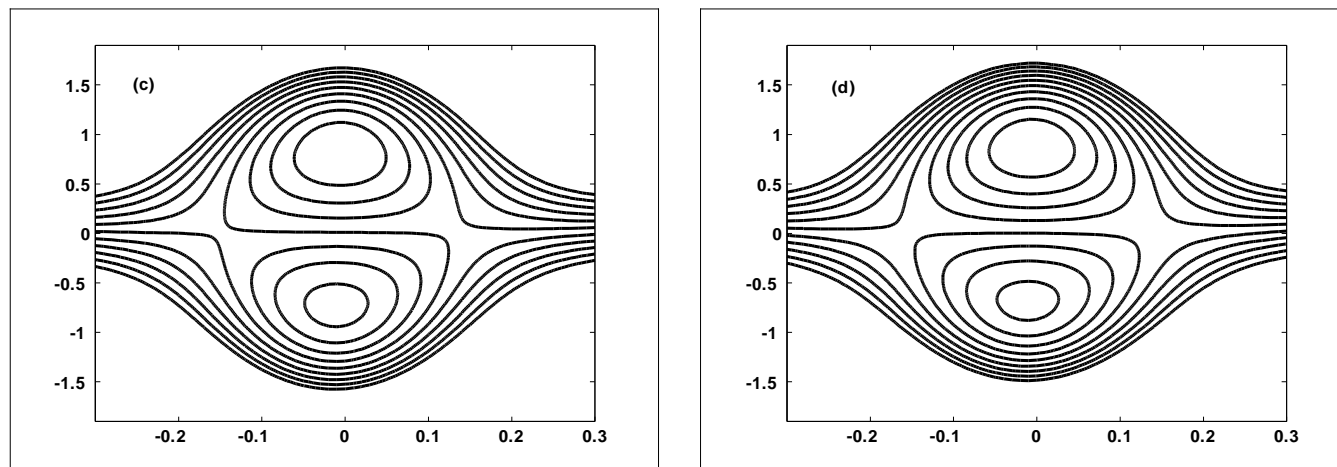


Figure 5. Stream lines for panels ((a) and (b)) for $\alpha = 0.2, 0.4$, ((c) and (d)) for $\beta = 0.1, 0.2$, while the other parameters are $b = 0.3, d = 1, a = 0.5, Q = -1, \phi = 0.3$.

(World Class University) program through the National Research Foundation of Korea (NRF) funded by the Ministry of Education, Science and Technology R31-2008-000-10049-0.

REFERENCES

- Akbar NS, Hayat T, Nadeem S, Hendi AA (2011). Effects of slip and heat transfer on the peristaltic flow of a third order fluid in an inclined asymmetric channel. *Int. J. Heat Mass Transf.*, 54:1654-1664.
- Ellahi R (2009). Steady and unsteady flow for newtonian and non-Newtonian fluids: Basics, concepts and methods". VDM Germany, 44(04): 352–357.
- Haroun MH (2007). Non-linear peristaltic flow of a fourth grade fluid in an inclined asymmetric channel. *Comput. Mater. Sci.*, 39:324-333.
- Hayat T, Javed M, Asghar S (2008). MHD peristaltic motion of Johnson-Segalman fluid in a channel with compliant walls. *Phys. Lett. A.*, 372: 5026-5036.
- Jaffrin MY, Shapiro AH (1971). Peristaltic pumping. *Annu. Rev. Fluid Mech.*, 3:13-16.
- Latham TW (1996). Fluid motion in a peristaltic pump. MS. Thesis, Massachusetts Institute of Technology, Cambridge.
- Mekheimer KS (2008). Effect of the induced magnetic field on peristaltic flow of a couple stress fluid. *Phys. Lett. A.*, 372: 4271-4278
- Mekheimer KS, Abd Elmaboud Y (2008). Influence of heat transfer and magnetic field on peristaltic transport of a Newtonian fluid in a vertical annulus. Application of an endoscope. *Phys. Lett. A*, 372(10): 1657–1665.
- Nadeem S, Akbar NS (2008). Influence of heat transfer on peristaltic transport of a Johnson-Segalman fluid in an inclined asymmetric channel, *Comm. Nonlinear Sci. Numer. Simul.*, 15: 2860-2877.
- Nadeem S, Akbar NS (2010). Series solutions for the peristaltic flow of a Tangent hyperbolic fluid in a uniform inclined tube, *Zeitschrift fur Naturforschung*, 65a: 887-895.
- Okosun KO, Makinde OD (2011). Modelling the impact of drug resistance in malaria transmission and its optimal control analysis, *Int. J. Phys. Sci.*, 6(28):6479-6487.
- Patel M, Timol MG (2010). The stress strain relationship for visco-inelastic non-Newtonian fluids, *Int. J. Appl. Math. Mech.*, 6(12): 79-93.
- Rico Garcia E, Soto Zarazua M, Alatorre-Jacome O, De La Torre-Gea GA, Gomez-Melendez DJ (2011). Aerodynamic study of greenhouses using computational fluid dynamics, *Int. J. Phys. Sci.*, 6(28): 6541-6547.
- Srinivas S, Gayathri R, Kothandapani M (2009). The influence of slip conditions, wall properties and heat transfer on MHD peristaltic transport. *Comput. Phys. Commun.*, 180: 2115-2122.
- Yildirim A, Sezer SA (2010). Effects of partial slip on the peristaltic flow of a MHD Newtonian fluid in an asymmetric channel. *Math. Comput. Model.*, 52: 618-625.